


 Cite this: *Mater. Chem. Front.*,  
2025, 9, 3495

# Flexible room-temperature-phosphorescence materials based on polymers with low glass-transition temperatures

 Bolun Huang,<sup>†a</sup> Yongfeng Zhang,<sup>†b</sup> Tao Wang,<sup>id b</sup> Baicheng Mei,<sup>id b</sup> Peng Sun,<sup>\*c</sup>  
Jianbing Shi,<sup>id b</sup> Bin Tong,<sup>id b</sup> Zitong Liu,<sup>id \*a</sup> Zhengxu Cai,<sup>id \*b</sup> and  
Yuping Dong,<sup>id b</sup>

Flexible room-temperature-phosphorescence (RTP) materials have attracted widespread attention due to their good stretchability, ease of deformation, and fatigue resistance. However, the stabilization of triplet excitons in RTP materials typically requires a crystalline or a rigid polymer matrix, which severely limits their mechanical flexibility at room temperature (300 K). To address this challenge, polymers with a glass-transition temperature ( $T_g$ ) below room temperature have emerged as a promising solution, offering a balance between matrix rigidification and efficient phosphorescence. Therefore, this review focuses on the recent development of flexible RTP polymers with low  $T_g$  (<300 K). It begins by exploring the fundamental trade-off between mechanical flexibility and long-lived RTP emission. Then, a comprehensive overview of the molecular design principles, processing strategies, and mechanistic insights for RTP materials with long lifetimes and high quantum yields is provided. Finally, the review summarizes the emerging applications of RTP materials in security information, stretchable displays, and wearable sensors, highlighting the transformative potential of these materials for next-generation flexible optoelectronics.

 Received 10th August 2025,  
Accepted 20th October 2025

DOI: 10.1039/d5qm00602c

[rsc.li/frontiers-materials](https://rsc.li/frontiers-materials)

## 1. Introduction

Room-temperature-phosphorescence (RTP) polymers have garnered intense interest due to their long-lived triplet emission<sup>1–5</sup> and broad applications, such as afterglow displays,<sup>6,7</sup> anti-counterfeiting inks,<sup>8</sup> time-resolved bio-imaging,<sup>9–12</sup> photodynamic therapy,<sup>13,14</sup> and mechano-/thermo-responsive sensors.<sup>15,16</sup> Traditionally, efficient organic RTP is achieved through crystallization,<sup>17</sup> host-guest doping,<sup>18,19</sup> or matrix rigidification,<sup>20–23</sup> all of which suppress the non-radiative decay of triplet excitons. The polymer matrix is becoming increasingly attractive as it can simultaneously play multiple roles in designing efficient RTP materials.<sup>24</sup> On the one hand, phosphors dispersed in a polymer matrix can avoid self-quenching, *e.g.*, triplet-triplet annihilation.<sup>25</sup> On the other hand, the rich diversity of polymer matrices allows the introduction of

properties such as mechanical flexibility and solution processability, which are essential for flexible and wearable optoelectronics.<sup>26,27</sup> Currently, the typical design strategy is to embed phosphors into a high-glass-transition-temperature (high- $T_g$ ) polymer matrix.<sup>28</sup> When the temperature is above  $T_g$ , the microscopic free volume is relatively large, resulting in enhanced mobility of polymer segments, which accelerates the molecular motions and hence induces non-radiative deactivation of triplet excitons.<sup>18,29</sup> However, when the temperature is lower than  $T_g$ , the negligible free volume severely limits the dynamic movement of polymer segments, leading to a significant reduction of the motion rate for organic molecules in the polymer matrix, thereby greatly prolonging triplet lifetimes and significantly improving the RTP quantum efficiency.<sup>30</sup> Therefore, most high-performance RTP polymers show a  $T_g$  value higher than room temperature, thus resulting in a reduction in their flexibility.<sup>31–35</sup> The polymer matrix that constitutes RTP materials must have sufficient chain mobility and macroscopic flexibility to ensure their practical application in the field of intrinsically flexible optoelectronic devices.<sup>36,37</sup> The polymer matrix with a  $T_g$  below room temperature has attracted much attention in recent years.<sup>38,39</sup>

In fact, ensuring that the matrix maintains rigidity at the microscopic level to reduce excitonic radiative transitions, while simultaneously preserving the high chain movement and radiative triplet excitons, is a trade-off feature, and how

<sup>a</sup> State Key Laboratory of Natural Product Chemistry, Key Laboratory of Special Function Materials and Structure Design, College of Chemistry and Chemical Engineering, Lanzhou University, Lanzhou 730000, China.  
E-mail: liuzt@lzu.edu.cn

<sup>b</sup> Beijing Key Laboratory of Construction Tailorable Advanced Functional Materials and Green Applications, School of Materials Science & Engineering, Beijing Institute of Technology, Beijing 100081, China. E-mail: caizx@bit.edu.cn

<sup>c</sup> School of Interdisciplinary Science, Beijing Institute of Technology, Beijing 100081, China. E-mail: sunpeng@bit.edu.cn

<sup>†</sup> These authors contributed equally to this work.

Table 1 The photophysical properties of low- $T_g$  RTP materials

RTP materials	Molecular weight (Da)	$T_g$ (K)	Measurements	$\lambda_p$ (nm)	$\tau_p$ (ms)	$\Phi_{RTP}$ (%)	Ref.
BPBA/PVDF	180 000 <sup>b</sup>	246.05	DSC, N <sub>2</sub>	485	1275.7	2.53	18
TpNP <sub>0.5</sub> @PU <sub>51</sub>	31 000 <sup>b</sup>	248.15	DSC, N/A	504	725	12.80	48
TEP3.5	80 000–300 000 <sup>a</sup>	218.15, 365.85	DSC, N/A	450, 547	344.8, 824.3	9.70	43
0.5 wt% 2Q5X/SIS	80 000–300 000 <sup>a</sup>	218.15, 365.85	DSC, air	500	1219	0.96	49
D1/SIS	64 000 <sup>b</sup>	211.35, 372.55	DSC, N <sub>2</sub>	500–520	630	12.90	41
D1/15 wt% PS/85 wt% PI	61 000 <sup>c</sup> , 220 000 <sup>d</sup>	211.15, 373.45	DSC, N <sub>2</sub>	500	310	N/A	41
RTP-CHS	38 500 <sup>a</sup>	216.52	DSC, N/A	490, 520	735, 414	3.57	50
CSE-R-P1	N/A	272.11	DSC, N <sub>2</sub>	420	31	6.86	51
CSE-R-P2	N/A	268.83	DSC, N <sub>2</sub>	520	294	1.97	51
CSE-R-P3	N/A	271.18	DSC, N <sub>2</sub>	630	101	9.47	51
BrNP <sub>2</sub> DMA <sub>79</sub> mTEGA <sub>19</sub>	5300 <sup>b</sup>	302.85	DSC, N <sub>2</sub>	583	6.1	6.60	29
BrBP <sub>2</sub> DMA <sub>79</sub> mTEGA <sub>19</sub>	N/A	NA	DSC, N <sub>2</sub>	500	1.59	3.20	29
PNB	54 800 <sup>b</sup>	298.15	DSC, N <sub>2</sub>	524	736	0.24	42
PNH	54 900 <sup>b</sup>	271.15	DSC, N <sub>2</sub>	524	691	0.20	42
PAPE	61 320 <sup>b,e</sup>	310.15	DSC, N <sub>2</sub>	548	232.25	1.21	36
PABE	68 800 <sup>b</sup>	298.15	DSC, N <sub>2</sub>	548	231.36	2.20	36
PAHE	N/A	268.15	DSC, N <sub>2</sub>	548	208.59	N/A	36
PVAc-PVPY-500	20 400 <sup>b,e</sup>	294.05	DSC, N <sub>2</sub>	680 <sup>f</sup>	200 <sup>g</sup>	N/A	52
CzPA <sub>0.10%</sub> -CO-PAM	N/A	263 <sup>h</sup>	DSC, N <sub>2</sub>	442	2550	32.60	53

<sup>a</sup>  $M_w$ . <sup>b</sup>  $M_n$ . <sup>c</sup> PS molecular weight. <sup>d</sup> PI molecular weight. <sup>e</sup> Molecular weight before alcoholysis. <sup>f</sup> Calculated using the equation:  $\lambda = 1240/T_1$ . <sup>g</sup> Approximate fitted lifetime in N<sub>2</sub>. <sup>h</sup> Approximate temperature.

to regulate this characteristic has become a major challenge.<sup>36,40</sup> Over the past five years, many molecular and supramolecular design strategies<sup>36,41–43</sup> have been employed to address this issue. Key advances include (i) dynamic non-covalent interactions that generate rigid microphases within a soft matrix, (ii) aggregation-induced phosphorescence luminogens whose emission is activated by nanoscale clustering in low- $T_g$  polymer hosts, and (iii) multicomponent doping systems in which a low- $T_g$  elastomer serves as the mechanical scaffold while a secondary rigid phase (nanoparticles,<sup>36,42</sup> crystalline domains,<sup>18,44</sup> or vitrified small-molecule clusters<sup>45,46</sup>) suppresses the triplet-exciton nonradiative process.

In this review, we first discuss the fundamental photophysical processes controlling triplet excitons in low- $T_g$  polymer matrices (Table 1) in Section 2, emphasizing the interrelationships between chain dynamics,<sup>18</sup> phase distribution,<sup>42</sup> and oxygen permeability.<sup>29</sup> We then divide flexible RTP systems into two categories in Section 3: (i) doped multicomponent matrices in which phosphors are dispersed in soft hosts and (ii) chemically engineered phosphorescent polymers with emissive backbones or side chains. Meanwhile, the relationship between the structural characteristics and RTP performance is also identified. In Section 4, by integrating insights from polymer physics, photophysics, and materials chemistry, a reasonable principle roadmap for next-generation flexible organic devices with both long-lived RTP and mechanical compliance is discussed. It is worth noting that since RTP gels have been the focus of recent related reviews,<sup>37,47</sup> it will not be included here.

## 2. Luminescence mechanism of RTP emission in low- $T_g$ matrices

The clarification of the underlying mechanism can provide guidance for the rational design of high-efficiency RTP materials

based on low- $T_g$  polymers. Low- $T_g$  polymers exhibit self-adapted intermolecular interactions that may shrink the motion range of the guest. From the perspective of aggregation science, the self-assembly state of the phosphor has a dominant impact on the resulting RTP performance.<sup>44</sup> Yang *et al.* have demonstrated this in an *N*-(4-cyanophenyl)carbazole (PCN) and styrene-isoprene-styrene block copolymer (SIS) system (Fig. 1a).<sup>43</sup> When a solution-processed film is prepared, PCN is molecularly dispersed within the SIS polymer matrix; the resulting RTP is monochromatic (approx. 450 nm) with a lifetime of 390 ms. Upon thermoplastic processing, PCN undergoes recrystallization within the elastomeric SIS scaffold. The reformed PCN microcrystals exhibit dual emission peaks at 450 nm and 540 nm, and the lifetime is extended to 830 ms. The significant enhancement results from the synergistic effect of cohesive elastic networks and rigid microcrystalline structures, which jointly suppress non-radiative decay pathways.

Special interactions, such as hydrogen bonding, are equally crucial for achieving efficient RTP in low- $T_g$  matrices (Fig. 1b).<sup>18,48,50–53</sup> Although polymer matrices, such as neat polyurethane (PU) and poly(vinylidene fluoride) (PVDF), have lower  $T_g$  values, the introduction of strong NH...HN or F...HO hydrogen-bonding arrays effectively enhances local rigidity, greatly extending triplet-state lifetimes and improving RTP efficiency. Actually, the addition of external nanofillers can further improve the performance of RTP materials (Fig. 1c).<sup>29</sup> For example, Tian *et al.* demonstrated that exfoliated nanoclay not only impedes non-radiative relaxation, but also establishes an oxygen barrier that hinders the diffusion of O<sub>2</sub>, resulting in a significant RTP efficiency. In addition, the crystallinity within the polymer matrix is a key structural parameter (Fig. 1d). In our recent work, we achieved tunability of the RTP characteristics by systematically adjusting the crystalline fraction of PVDF.<sup>18</sup> Low crystallinity in conjunction with high  $\alpha$ -phase content was identified as the ideal choice for optimizing RTP performance.

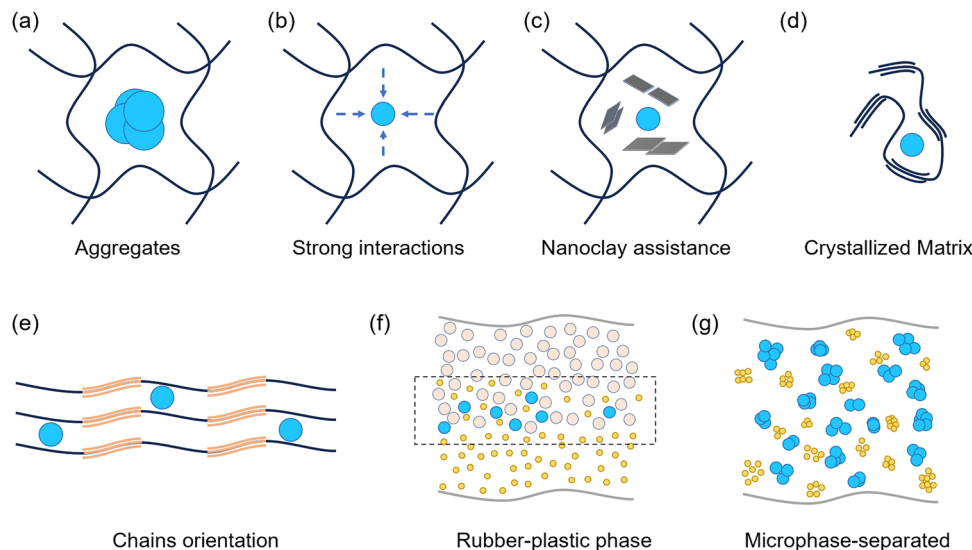


**Fig. 1** The mechanisms for the design of RTP materials based on low- $T_g$  polymers: (a) aggregated phosphors in a polymer matrix; (b) strong intermolecular interactions; (c) external nanoclay assistance; (d) crystallized polymer matrix; (e) polymer chain orientation; (f) plastic–rubber phase interface; and (g) microphase separation.

Moreover, mechanical stretching has been identified as another mechanically induced strategy to improve RTP performance (Fig. 1e).<sup>48</sup> When polymer materials undergo macroscopic elongation, their microscopic flexible chains become highly oriented and densely packed, which significantly increases the local rigidity of the force-induced microcrystalline region, thereby suppressing non-radiative relaxation pathways. In multicomponent polymer matrices, phase separation inevitably generates well-defined interfaces.<sup>49</sup> As illustrated in Fig. 1f, phosphors located in either the rubbery domain or the glassy domain may not restrict the molecular motion, resulting in the non-radiative decay of triplet excitons. In contrast, phosphors precisely positioned at the rubber-plastic interface benefit from the interfacial microenvironment, with their combined rigidity and limited mobility effectively stabilizing the emission triplet state. Finally, block copolymers naturally self-assemble into periodic, nanoscale microphases.<sup>36,41–43</sup> In the typical SIS system (Fig. 1g), the hard styrene segments furnish a rigid scaffold for the phosphor, while the soft isoprene segments maintain macroscopic flexibility. This collaborative architecture—regular microphase separation coupled with spatially selective phosphor localization—provides a robust platform for achieving high RTP efficiency and mechanical compliance simultaneously. In short, achieving both high-performance phosphorescence and flexibility in materials presents a significant challenge. High-performance phosphorescence requires a rigid molecular environment to minimize non-radiative transitions and to enhance the emission efficiency. However, flexibility necessitates molecular mobility to allow deformation without compromising the material's integrity. Balancing these seemingly contradictory requirements is crucial for developing high-performance flexible phosphorescent materials.

### 3. Construction strategies for RTP materials based on low- $T_g$ polymers

RTP materials based on low- $T_g$  polymers can be categorized into two major systems: physical mixing and chemical linking. In the physical mixing category, RTP is achieved by dispersing phosphors into low- $T_g$  polymer matrices, with performance influenced by host–guest interactions and matrix microstructures, including (1) single-component low- $T_g$  polymers, (2) microphase-separated block copolymers, and (3) multi-component elastomers. In the chemical linking category, RTP is achieved by covalently incorporating phosphorescent units into polymer chains *via* copolymerization.

#### 3.1. Physically mixed phosphors and polymers

**3.1.1. Single-component low- $T_g$  polymer matrices.** A strong interaction between the phosphor and polymer matrix is generally required to realize RTP emissions. Recently, our group developed a flexible RTP material with poly(vinylidene fluoride) (PVDF;  $M_n = 180\,000$  Da,  $T_g = 246.05$  K) as the matrix (Fig. 2a).<sup>18</sup> When 4-biphenylboronic acid (BPBA) is used as the emissive dopant, the robust hydrogen-bonded network between BPBA and PVDF, and the controllable crystallinity and elevated  $\alpha$ -polymorph content of PVDF synergistically limit the radiative decay of triplet excitons and extend the phosphorescence lifetime. The resulting BPBA/PVDF film exhibits emission at 485 nm with a long lifetime of 1.28 s and a  $\Phi_{\text{RTP}}$  of 2.53%. Consistent with the intrinsic flexibility of PVDF, the film retains stable RTP even after 20 000 bending cycles and can be readily folded or stretched. Therefore, although the composite material exhibits low overall crystallinity, it has a high  $\alpha$ -phase fraction required for efficient RTP, which provides the microwave-responsive emission (2.45 GHz) and hence enables dynamic optical modulation.

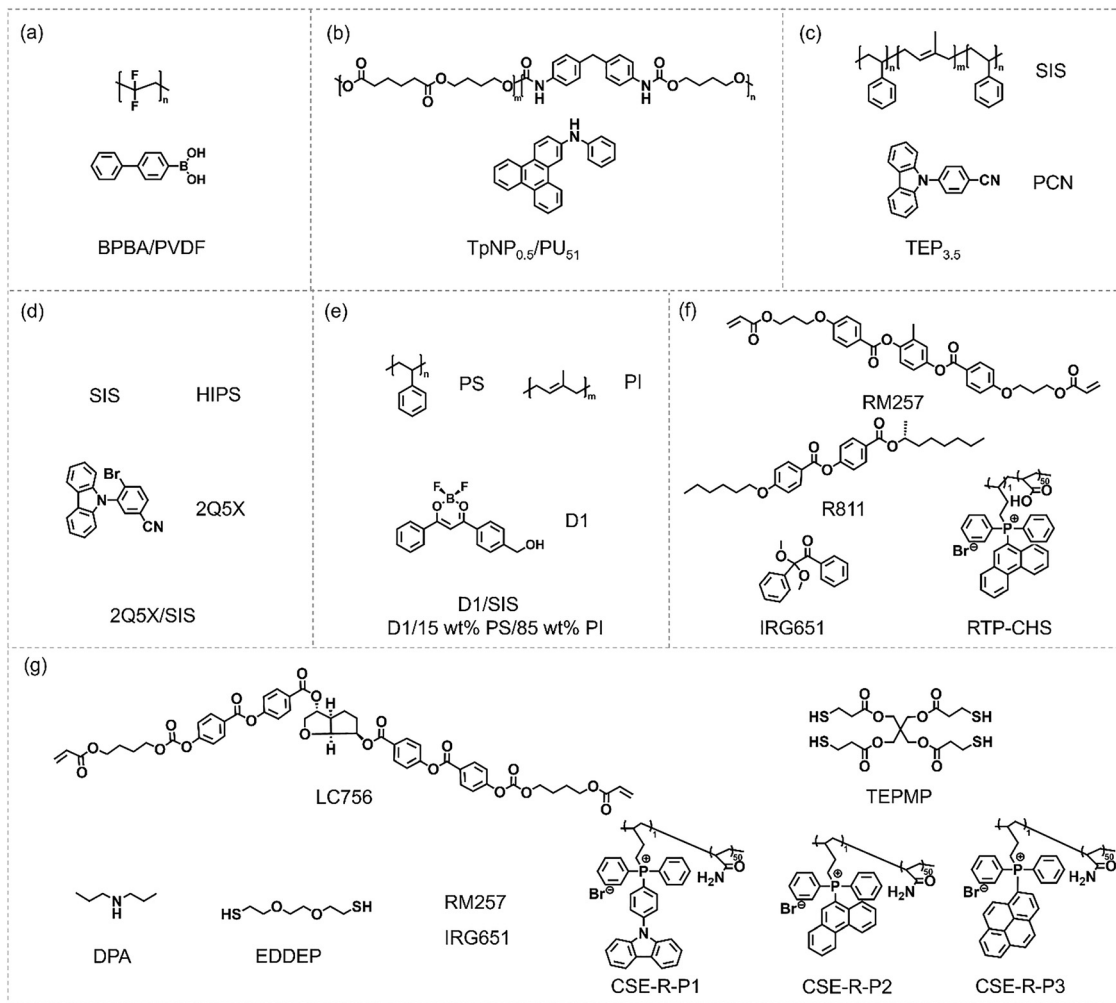


Fig. 2 The chemical structures of phosphors and the doped polymer matrices.

In 2024, Yang *et al.* developed a mechano-responsive RTP system by dispersing the triphenylene derivative TpNP (0.5 wt%) in a commercial PU elastomer (Fig. 2b).<sup>48</sup> PU is composed of hard segments of 4,4'-diphenylmethane diisocyanate and polycaprolactone (51 wt%;  $T_g = 248.15$  K) and soft segments of poly(1,4-butylene adipate) diol. Hydrogen bonding between the hard segments and the TpNP amine substituents, as well as the  $\pi$ - $\pi$  interactions between aromatic hard segments and the triphenylene core, rigidifies the local environment and hence suppresses non-radiative decay. As a result, TpNP<sub>0.5</sub>@PU<sub>51</sub> emits at 504 nm with an initial lifetime of 37 ms and a  $\Phi_{\text{RTP}}$  of 6.6%. Macroscopic mechanical stretching induces microscopic chain orientation and increases the corresponding local polarity and immobility of stretched domains, boosting the lifetime and  $\Phi_{\text{RTP}}$  to 725 ms and 12.5%, respectively. Due to the reversible microphase-separated architecture of PU<sub>51</sub>, this mechano-RTP response persists without fatigue over 500 loading/unloading cycles.

**3.1.2. Microphase-separated block-copolymer matrices.** Embedding phosphors into elastomeric matrices is a straightforward route to obtain flexible RTP materials, but suppression of non-radiative decay caused by intense segmental motion

of low- $T_g$  chains remains remarkable. Block copolymers that undergo microphase separation to form rigid nanodomains dispersed in a continuous rubbery phase provide an elegant solution. The styrene-isoprene-styrene (SIS) triblock copolymer is a system explored for this purpose. SIS is a commercial thermoplastic elastomer, in which the glassy polystyrene (PS) end-blocks aggregate into nanoscale hard domains, while the rubbery polyisoprene (PI) mid-blocks form the continuous soft matrix. This nanocomposite-like architecture endows the material with room-temperature elasticity and high-temperature melt processability, offering both mechanical compliance and spatial confinement for triplet emitters.

In 2022, Yang *et al.* reported TEP<sub>3.5</sub>-SIS doped with 3.5 wt% phosphor PCN (Fig. 2c).<sup>43</sup> The molecular weight of SIS is 80 000–300 000 Da, and its  $T_g$  is 218.15 K for PI and 365.85 K for PS. After *in situ* oxygen consumption under 365 nm irradiation (10 s), the film emitted dual RTP peaks at 450 and 547 nm with lifetimes of 345 ms and 824 ms, respectively, and a  $\Phi_{\text{RTP}}$  of 9.7%. During thermoplastic processing, PCN recrystallizes within PS nanodomains. Therefore, the rigid PS cages suppress non-radiative motions, while the PI phase maintains the

macroscopic stretchability (>300% strain) and autonomous self-recovery of the material. Subsequently, based on this platform, Yang *et al.* further introduced 2Q5X (0.5 wt%) into both SIS and high-impact polystyrene (HIPS) (Fig. 2d).<sup>49</sup> HIPS is a PS matrix toughened by dispersed polybutadiene (PB) rubber particles, again providing PS/PB interfacial confinement. The optimized 2Q5X/SIS film reaches 59 lux peak brightness and 1.22 s lifetime ( $\Phi_{\text{RTP}} = 0.96\%$ ), whereas 2Q5X/HIPS delivered 34 lux and 1.09 s. Spatially resolved spectroscopy revealed that triplet excitons are localized at the PS–rubber interface, where internal stress and reduced free volume jointly suppress vibrational deactivation.

Recently, Wen *et al.* conducted a systematic comparison of phosphor D1 dispersed in (i) a 15 wt% PS/85 wt% PI physical blend and (ii) a PS-*b*-PI (SIS) block copolymer (Fig. 2e),<sup>41</sup> with their corresponding  $T_g$  values being 211.35 K and 211.15 K. The molecular weights of SIS, PS, and PI are 64 000, 61 000, and 220 000 Da, respectively. Both the 15 wt% PS/85 wt% PI blend and the SIS matrix exhibit microphase separation. Due to these microphase-separation structures, both D1/PS/PI and D1/SIS emit at approximately 500 nm but with lifetimes of 310 ms and 630 ms, respectively. The  $\Phi_{\text{RTP}}$  of D1/SIS reaches 12.9%. Notably, the RTP material performance of D1/SIS is superior to that of D1/PS/PI. The authors attribute this enhancement to the size and uniformity of the microphase-separation domains: the large, irregular aggregates formed in PS/PI blends can only offer inefficient RTP, while the well-defined nanodomains in the SIS matrix significantly extend the lifetime of RTP emission and improve brightness.

**3.1.3. Multicomponent elastomer matrices.** In 2024, Zhao *et al.* reported on the circularly polarized RTP (CP-RTP) achieved by employing the polymer itself as the emissive dopant (Fig. 2f).<sup>50</sup> They synthesized the phosphonium-functionalized copolymer but-3-en-1-yl(phenanthren-9-yl)diphenylphosphonium bromide-*co*-acrylic acid ( $M_w = 38\,500$  Da) and embedded it (5 wt%) into a multicomponent matrix composed of a nematic liquid crystal (LC), the reactive mesogen RM257, the photoinitiator IGR651, and the chiral dopant R811, thereby obtaining the composite RTP-CHS. The LC phase exhibits a  $T_g$  value of 216.52 K. Within this architecture, the rigid polymer network severely restricts intramolecular motion, while ionic and dipolar interactions further suppress the non-radiative decay of triplet excitons. Consequently, dual RTP bands centered at 490 nm and 520 nm are observed, with lifetimes of 735 ms and 414 ms, respectively, and an overall quantum yield of 3.57%. Most importantly, the combination of the RTP polymer and the chiral helical superstructure results in abnormal circular polarization, achieving an asymmetry factor ( $g_{\text{lum}}$ ) of 1.49.

Furthermore, Zhao *et al.* subsequently demonstrated that flexible CP-RTP can be achieved in low- $T_g$  matrices.<sup>51</sup> In this study (Fig. 2g), they prepared a series of chiral superstructure elastomers (CSEs) by photopolymerizing (365 nm, 10 min) mixtures of the chiral dopant LC756, LC monomer RM257, photoinitiator IRG651, catalyst DPA, cross-linker PETMP, chain extender EDDT, and one of three RTP-active polymers (P1, P2, and P3). The resulting CSE-R-P1, CSE-R-P2, and CSE-R-P3

composite materials exhibit tunable afterglow across the visible spectrum: 420 nm (blue), 520 nm (green), and 630 nm (red) with lifetimes of 31 ms, 294 ms, and 101 ms and the corresponding  $\Phi_{\text{RTP}}$  values of 6.86%, 1.97%, and 9.47%, respectively. As the  $T_g$  values of these CSE-RTP films are between 268.83 K and 272.11 K, they are able to maintain significant flexibility and elasticity at room temperature. For example, CSE-R-P3 exhibits a fracture elongation of 110% and a Young's modulus of 0.88 MPa. Such mechanical compliance makes these materials particularly attractive for manufacturing soft optoelectronic devices, including wearable sensors, flexible displays, and dynamically reconfigurable optical encryption tags.

### 3.2. Chemically linked phosphors and polymers

RTP polymers with inherent flexibility can also be developed through homopolymerization or free-radical copolymerization. In 2021, Tian *et al.* reported an intrinsically flexible RTP polymer obtained through one-step free-radical copolymerization (Fig. 3a).<sup>29</sup> By adopting the 4-bromo-1,8-naphthalic anhydride (BrNpA) derivative as the emissive unit, they synthesized BrNpA<sub>2</sub>DMA<sub>79</sub>mTEGA<sub>19</sub> ( $M_n = 5300$  Da,  $T_g = 302.85$  K). When 0.5 wt% NHT nanoclay was added, followed by oxygen depletion, oxygen barriers hindered O<sub>2</sub> diffusion, resulting in the formation of a composite material that emits at 583 nm with a lifetime of 6.1 ms and a  $\Phi_{\text{RTP}}$  of 6.60%. In the same work, an analogous approach but with the use of 4'-bromo-[1,1'-biphenyl]-4-yl acrylate (BrBp) was adopted to prepare the BrNpA<sub>2</sub>DMA<sub>79</sub>mTEGA<sub>19</sub> film, which exhibited flexibility, foldability, and cuttability without brittleness under low- $T_g$  and nanoconfined conditions. In 2024, Gu and An developed low- $T_g$  block copolymers PNB and PNH (Fig. 3b), which contain rigid PAA and flexible PBMB (binaphthol-phosphorus) segments with  $T_g$  values of PNB and PNH being 298.15 K and 271.15 K, respectively.<sup>42</sup> Microphase separation and self-assembly immobilize the phosphors, resulting in 524 nm RTP emission with lifetimes of 736 ms and 691 ms and the corresponding  $\Phi_{\text{RTP}}$  values of 0.24% and 0.20% for PNB and PNH, respectively. The flexible-segment proportion was adjusted to achieve a stretchable display that emits continuous green light, which sustains elongations up to 600% and maintains RTP after repeated folding.

Gu and An also reported a series of copolymers, PAPE, PABE, and PAHE, which were prepared *via* two-step radical polymerization followed by hydrolysis (Fig. 3c).<sup>36</sup> Their  $T_g$  values are 310.15 K, 298.15 K, and 268.15 K and lifetimes are 232.3 ms, 231.4 ms, and 208.6 ms, respectively, at a common emission wavelength of  $\sim 548$  nm and  $\Phi_{\text{RTP}}$  spanning 1.21–2.20%. It is remarkable that the PABE film can elongate up to 650% while maintaining its high RTP brightness, highlighting the synergistic effect between low- $T_g$  polymer matrices and microphase-separated architectures in simultaneously achieving flexibility and persistent room-temperature phosphorescence. It is noteworthy that the phosphorescence lifetime exhibits an inverse correlation with substituent chain length:  $\tau$  decreases from 232.3 ms to 208.6 ms as the alkyl spacer increases from 2 to 5 carbons. This trend is mirrored by a monotonic drop in  $T_g$ ,

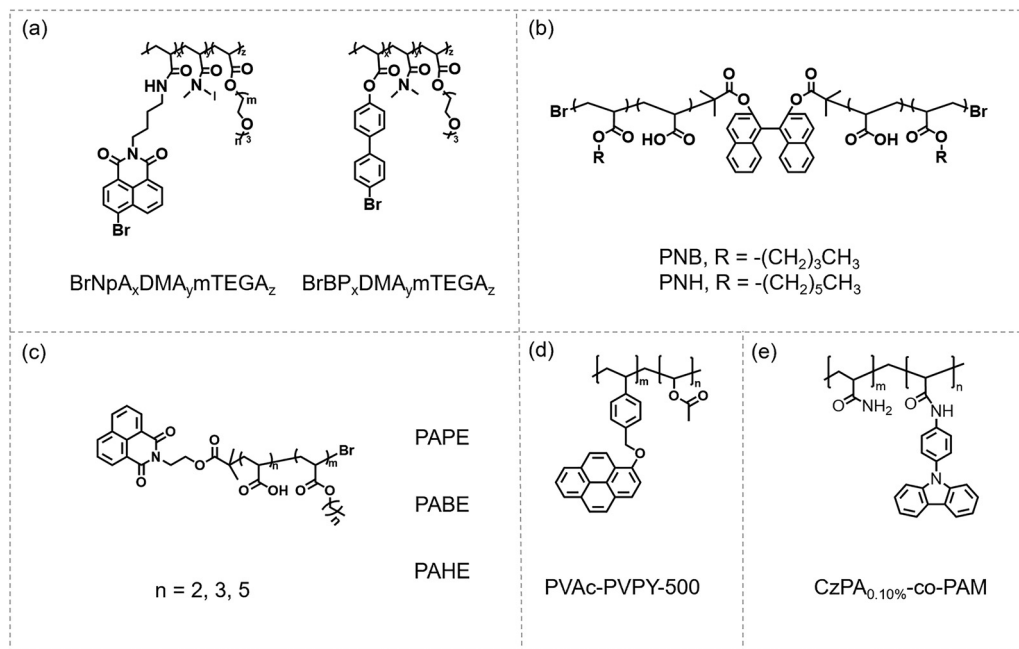


Fig. 3 The chemical structures of the synthetic RTP polymers.

indicating that longer side chains intensify segmental mobility. Consequently, the short substituents restrict polymer-chain motion and foster uniform rigid micro-domains that suppress non-radiative triplet exciton decay, whereas the long substituents promote chain movement and dilute chromophore aggregation.

Additionally, Yang *et al.* disclosed a vinyl acetate–pyrene copolymer, PVAc-PVPY-500 ( $M_n = 20\,400$  Da,  $T_g = 294.05$  K; Fig. 3d), synthesized *via* free-radical copolymerization.<sup>52</sup> Due to the absence of hydrogen-bonding networks, PVAc-PVPY-500 is non-phosphorescent. One-step alcoholysis converts it into PVA-PVPY-500, which has an ultra-long RTP lifetime of 498 ms and a  $\Phi_{\text{RTP}}$  of 0.2% at 498 nm. The dip-coating of cotton fibers with an aqueous PVA-PVPY solution can generate mechanically flexible RTP fibers. Meanwhile, Lu *et al.* reported a carbazole–acrylamide copolymer, CzPA<sub>0.10%</sub>-co-PAM ( $M_n$  not specified,  $T_g \approx 263$  K; Fig. 3e), which was obtained by free-radical copolymerization of 4-(9*H*-carbazol-9-yl)aniline (CzPA) and acrylamide.<sup>53</sup> The polymer exhibits 442 nm RTP with a lifetime of 2.55 s and a  $\Phi_{\text{RTP}}$  of 32.6%, but its RTP can be rapidly quenched by atmospheric moisture. The acidic hydrolysis (HCl) of amide side chains produces carboxylic acids and triggers phase separation to obtain H-CzPA0. The RTP lifetime of the 10%-co-PAM hydrogel is 503 ms. The prepared hydrogel displays a tensile strength of 5.1 MPa, an elongation at break of 452%, a toughness of  $19.3 \text{ MJ m}^{-3}$ , and a water stability of > 30 days, thereby exhibiting high RTP efficiency as well as mechanical robustness and environmental durability.

## 4. Applications

Low- $T_g$  polymers have become a platform for balancing mechanical compliance with long-lived RTP. Based on the

complementary strategies, researchers have achieved stretchable, foldable and even self-healing RTP materials with lifetimes of over 1 s and a quantum yield of over 10%. These advances made it possible to demonstrate stretchable displays, wearable sensors, mechano- and microwave-responsive films, underwater encryption and continuous RTP fibers. By incorporating low- $T_g$  polymers with color-tunable RTP emitters, researchers have developed luminescent patterns featuring mechanical compliance, thus enabling flexible displays (Fig. 4a).<sup>36</sup> This breakthrough addresses the inherent limitations of conventional rigid RTP display devices and delivers a material solution that combines “long-lasting luminescence” with “mechanical durability” for next-generation flexible display technologies. Ultrathin RTP films can be integrated into wearable devices through lamination (Fig. 4b).<sup>48</sup> This configuration enables information control *via* simple finger-rolling gestures, creating intuitive human–robot interfaces. The system operates without complex circuitry, relying exclusively on dynamic responses from RTP optical signals to achieve an intuitive and lightweight interactive platform. These characteristics enable its successful application in stress detection and motion monitoring.

The exceptional oxygen permeability of low- $T_g$  polymer matrices enables effective triplet emission quenching, which is a principle harnessed in compact oxygen sensor design (Fig. 4c).<sup>29</sup> Operating without complex detection modules, these sensors achieve rapid and precise oxygen monitoring exclusively through real-time tracking of RTP signal dynamics. This approach simultaneously delivers high sensitivity and mechanical conformability in oxygen sensing applications. Stretchable RTP polymers exhibit dual modulation of emission color and lifetime under cyclic stretching, achieving

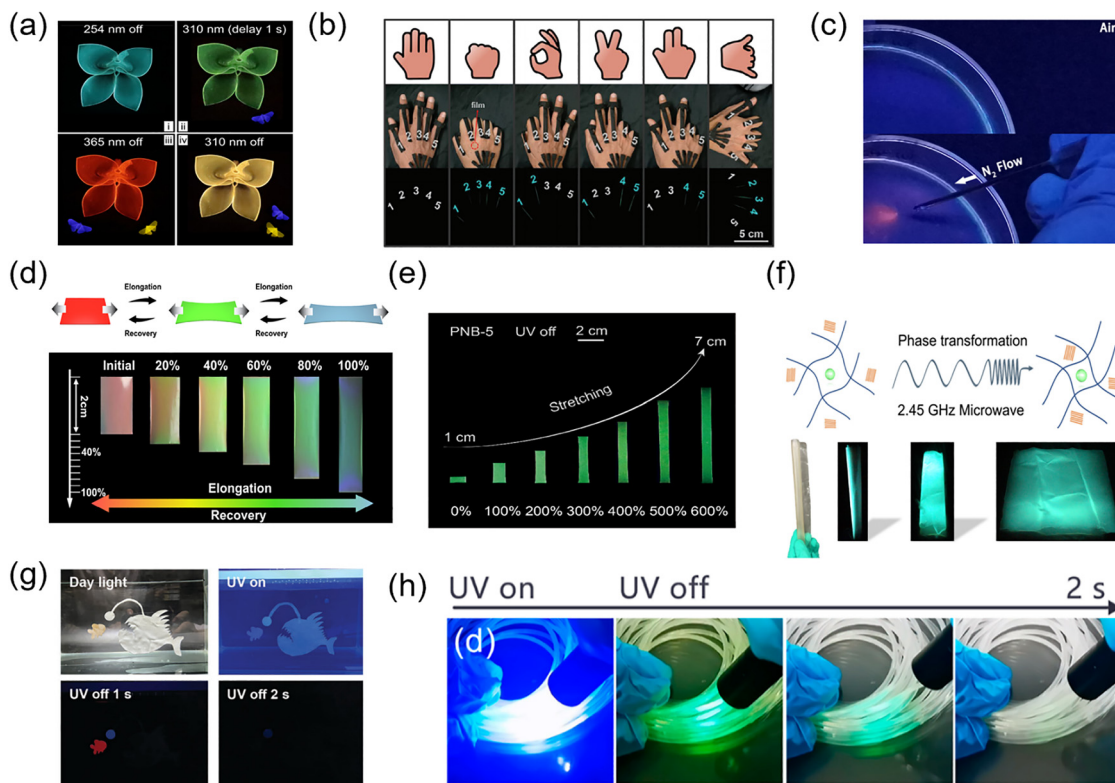


**Fig. 4** Typical applications of low- $T_g$  RTP polymeric materials. (a) Display of multiple colorful afterglow.<sup>36</sup> Copyright 2024 Springer Nature. (b) Human-robot wearable devices.<sup>48</sup> Copyright 2025 John Wiley and Sons. (c) Nitrogen sensor.<sup>29</sup> Copyright 2020 John Wiley and Sons. (d) and (e) Stretchable and mechano-responsive RTP polymers.<sup>42,51</sup> Copyright 2025 John Wiley and Sons and Copyright 2024 American Chemical Society. (f) Microwave-responsive RTP film.<sup>18</sup> Copyright 2023 John Wiley and Sons. (g) Underwater information encryption.<sup>53</sup> Copyright 2024 John Wiley and Sons. (h) Scalable RTP fiber.<sup>41</sup> Copyright 2024 American Chemical Society.

remarkable elongation up to 600% without compromising functional integrity (Fig. 4d–e).<sup>42,51</sup> Such exceptional mechanical responsiveness enables their use as light-emitting layers for stretchable optical displays, suitable for wearable optical devices and flexible 3D display systems. The incorporation of crystalline domains within the polymer matrix enables microwave activation at 2.45 GHz, simultaneously enhancing both the phosphorescence lifetime and quantum yield (Fig. 4f).<sup>18</sup> This capability facilitates non-contact manipulation of RTP emission, allowing microwave-selective detection of optical excitation.

Underwater information encryption has also been successfully validated using spectrally unique RTP signatures (Fig. 4g).<sup>53</sup> This technology can be utilized for temporary underwater information storage and transmission, such as anti-counterfeiting labels for subaquatic equipment and temporary data tagging. By emulating the dynamic coloration mechanisms of cephalopods, these systems achieve adaptive camouflage through precise regulation of RTP emission spectra to match underwater optical conditions. RTP fibers produced by the scalable high-throughput processing present a viable solution for large-scale implementation of multifunctional materials systems (Fig. 4h).<sup>41</sup> The versatility of these fibers enables diverse applications, such as woven flexible luminescent textiles for smart apparel safety features and large-scale optical fiber arrays serving as backlight components for flexible

displays and architectural luminous elements. This manufacturing approach effectively bridges the gap between laboratory research and industrial application for low- $T_g$  polymer-based RTP materials. Overall, the strategic integration of low- $T_g$  polymers with color-tunable RTP emitters has enabled a new generation of functional systems. These developments not only overcome the intrinsic brittleness and rigidity of conventional RTP systems but also provide innovative technological pathways for flexible optoelectronics.

## 5. Summary and outlook

The rapid progress in flexible RTP materials has generated significant scientific interest in low- $T_g$  polymers.<sup>37,54–57</sup> The development of flexible polymer-based RTP materials still faces the challenge of achieving a balance between macroscopic flexibility and triplet exciton stability. Addressing this challenge requires advancements, including molecular design, processing methodologies, and structural engineering. First, molecular design should focus on architectures that combine flexible backbones with rigid micro-domains, utilizing dynamic non-covalent interactions and tailoring copolymer compositions to optimize the balance between softness and efficiency. Second, processing methodologies should enable precise

microstructural control through techniques such as thermo-plastic forming and *in situ* nanoclay exfoliation, which help minimize nonradiative decay and oxygen quenching. Third, structural engineering needs to exploit the intrinsic multi-phase characteristics of the materials by optimizing rubber-plastic interfaces, utilizing block copolymer phase separation, and designing microcrystal-elastic networks to create environments that combine macroscopic flexibility with microscopic rigidity. For future applications in soft optoelectronics, integrated innovation across these technical domains is essential. This must be combined with scalable manufacturing solutions and robust environmental durability to ensure practical and reliable implementation.

The future development of low- $T_g$  polymer-based flexible RTP materials should meet the requirements of multifunctional integrated applications, necessitating materials that exhibit environmental stability and high RTP performance. In addition, fabricating flexible RTP systems using ultra-low- $T_g$  polymer matrices remains fundamentally challenging, largely due to the intrinsic trade-off between the high chain mobility of soft matrices and the immobilization necessary for triplet exciton stabilization. Thus, the simultaneous achievement of high flexibility, long lifetime, and elevated quantum yield in ultra-low  $T_g$  polymer hosts represents a crucial objective. Current studies mainly focus on mitigating non-radiative decay through polymer matrix design; future work should place greater emphasis on understanding how polymer dielectric properties influence electron density redistribution in phosphorescent centers and strategically coordinating these with critical parameters like free volume to improve RTP performance. The external heteroatoms and heavy atoms may promote the ISC process of the phosphorescent molecules. Additionally, continuing simplification of synthesis procedures is essential to enable scalable production and hasten industrial integration in emerging sectors, such as flexible electronics and photonic displays. By deeply integrating rational molecular design with innovative processing methodologies, flexible RTP materials are expected to advance from laboratory exploration to practical technological deployment.

## Author contributions

B. Huang and Y. Zhang prepared the manuscript under the supervision of Z. Cai and Y. Dong. T. Wang, B. Mei, and P. Sun revised this manuscript. All authors contributed to the general discussion.

## Conflicts of interest

The authors declare that they have no known competing financial interests or personal relationships that could have appeared to influence the work reported in this paper.

## Data availability

No new data were generated or analyzed in this review. Data sharing is not applicable to this article.

## Acknowledgements

This work was financially supported by the National Natural Science Foundation of China (22222501, 52473290, 22375080, and 22175081), the Natural Science Foundation of Beijing Municipality (2232022, 2242060, and 2252054), and the Natural Science Foundation of Hebei Municipality (B2025105007 and B2025105009).

## References

- 1 G. Zhang, G. M. Palmer, M. W. Dewhirst and C. L. Fraser, A Dual-emissive-materials Design Concept Enables Tumour Hypoxia Imaging, *Nat. Mater.*, 2009, **8**, 747–751.
- 2 D. Lee, O. Bolton, B. C. Kim, J. H. Youk, S. Takayama and J. Kim, Room Temperature Phosphorescence of Metal-free Organic Materials in Amorphous Polymer Matrices, *J. Am. Chem. Soc.*, 2013, **135**, 6325–6329.
- 3 M. S. Kwon, D. Lee, S. Seo, J. Jung and J. Kim, Tailoring Intermolecular Interactions for Efficient Room-temperature Phosphorescence from Purely Organic Materials in Amorphous Polymer Matrices, *Angew. Chem., Int. Ed.*, 2014, **53**, 11177–11181.
- 4 Y. Su, S. Z. F. Phua, Y. Li, X. Zhou, D. Jana, G. Liu, W. Q. Lim, W. K. Ong, C. Yang and Y. Zhao, Ultralong Room Temperature Phosphorescence from Amorphous Organic Materials toward Confidential Information Encryption and Decryption, *Sci. Adv.*, 2018, **4**, eaas9732.
- 5 L. Gu, H. Wu, H. Ma, W. Ye, W. Jia, H. Wang, H. Chen, N. Zhang, D. Wang, C. Qian, Z. An, W. Huang and Y. Zhao, Color-tunable Ultralong Organic Room Temperature Phosphorescence from a Multicomponent Copolymer, *Nat. Commun.*, 2020, **11**, 944.
- 6 C. Lin, Z. Wu, H. Ma, J. Liu, S. You, A. Lv, W. Ye, J. Xu, H. Shi, B. Zha, W. Huang, Z. An, Y. Zhuang and R. Xie, Charge Trapping for Controllable Persistent Luminescence in Organics, *Nat. Photonics*, 2024, **18**, 350–356.
- 7 W. Dai, G. Li, Y. Zhang, Y. Ren, Y. Lei, J. Shi, B. Tong, Z. Cai and Y. Dong, Controllable Modulation of Efficient Phosphorescence through Dynamic Metal-Ligand Coordination for Reversible Anti-Counterfeiting Printing of Thermal Development, *Adv. Funct. Mater.*, 2023, **33**, 2210102.
- 8 Y. Zhang, Z. Wang, Y. Su, Y. Zheng, W. Tang, C. Yang, H. Tang, L. Qu, Y. Li and Y. Zhao, Simple Vanilla Derivatives for Long-Lived Room-Temperature Polymer Phosphorescence as Invisible Security Inks, *Research*, 2021, **2021**, 8096263.
- 9 J. Yang, Y. Zhang, X. Wu, W. Dai, D. Chen, J. Shi, B. Tong, Q. Peng, H. Xie, Z. Cai, Y. Dong and X. Zhang, Rational Design of Pyrrole Derivatives with Aggregation-Induced Phosphorescence Characteristics for Time-Resolved and Two-Photon Luminescence Imaging, *Nat. Commun.*, 2021, **12**, 4883.
- 10 F. Xiao, H. Gao, Y. Lei, W. Dai, M. Liu, X. Zheng, Z. Cai, X. Huang, H. Wu and D. Ding, Guest-host Doped Strategy for Constructing Ultralong-Lifetime Near-Infrared Organic

- Phosphorescence Materials for Bioimaging, *Nat. Commun.*, 2022, **13**, 186.
- 11 Y. Zhao, J. Yang, C. Liang, Z. Wang, Y. Zhang, G. Li, J. Qu, X. Wang, Y. Zhang, P. Sun, J. Shi, B. Tong, H. Y. Xie, Z. Cai and Y. Dong, Fused-Ring Pyrrole-Based Near-Infrared Emissive Organic RTP Material for Persistent Afterglow Bioimaging, *Angew. Chem., Int. Ed.*, 2024, **63**, e202317431.
  - 12 L. Kang, C. Chao, C. Xiong, S. Yu, C. Xiao, C. Zhao, S. Cui, J. Li, J. Li, J. Shi, B. Tong, Z. Wang, Y. Song, W. Zhao, Z. Cai and Y. Dong, Host-Guest Strategy for Organic Phosphorescence to Generate Oxygen Radical over Singlet Oxygen, *Chem. Mater.*, 2024, **36**, 7332–7342.
  - 13 J. Huang, L. Su, C. Xu, X. Ge, R. Zhang, J. Song and K. Pu, Molecular Radio Afterglow Probes for Cancer Radiodynamic Theranostics, *Nat. Mater.*, 2023, **22**, 1421–1429.
  - 14 D. Liu, W.-J. Wang, P. Alam, Z. Yang, K. Wu, L. Zhu, Y. Xiong, S. Chang, Y. Liu, B. Wu, Q. Wu, Z. Qiu, Z. Zhao and B. Z. Tang, Highly Efficient Circularly Polarized Near-Infrared Phosphorescence in both Solution and Aggregate, *Nat. Photonics*, 2024, **18**, 1276–1284.
  - 15 Y. Wang, Z. Xiong, Y. Wang, A. Li, Y. Fang, L. Li, K. Wang, Q. Li and H. Zhang, Pressure-Engineered Through-Space Conjugation for Precise Control of Clusteroluminescence, *Angew. Chem., Int. Ed.*, 2024, e202420502.
  - 16 W. Dai, X. Niu, X. Wu, Y. Ren, Y. Zhang, G. Li, H. Su, Y. Lei, J. Xiao, J. Shi, B. Tong, Z. Cai and Y. Dong, Halogen Bonding: A New Platform for Achieving Multi-Stimuli-Responsive Persistent Phosphorescence, *Angew. Chem., Int. Ed.*, 2022, **61**, e202200236.
  - 17 W. Feng, D. Chen, Y. Zhao, B. Mu, H. Yan and M. Barboiu, Modulation of Deep-Red to Near-Infrared Room-Temperature Charge-Transfer Phosphorescence of Crystalline “Pyrene Box” Cages by Coupled Ion/Guest Structural Self-Assembly, *J. Am. Chem. Soc.*, 2024, **146**, 2484–2493.
  - 18 Y. Zhang, W. Zhang, J. Xia, C. Xiong, G. Li, X. Li, P. Sun, J. Shi, B. Tong, Z. Cai and Y. Dong, Microwave-Responsive Flexible Room-Temperature Phosphorescence Materials Based on Poly(vinylidene fluoride) Polymer, *Angew. Chem., Int. Ed.*, 2023, **62**, e202314273.
  - 19 Y. Zhang, C. Xiong, W. Wang, W. Dai, Y. Ren, J. Xia, G. Li, J. Shi, B. Tong, X. Zheng, X. Shao, Z. Cai and Y. Dong, Wide-Range Color-Tunable Afterglow Emission by the Modulation of Triplet Exciton Transition Processes Based on Buckybowl Structure, *Aggregate*, 2023, **4**, e310.
  - 20 Q. Chen, L. Qu, H. Hou, J. Huang, C. Li, Y. Zhu, Y. Wang, X. Chen, Q. Zhou, Y. Yang and C. Yang, Long Lifetimes White Afterglow in Slightly Crosslinked Polymer Systems, *Nat. Commun.*, 2024, **15**, 2947.
  - 21 Y. Cao, D. Wang, Y. Zhang, G. Li, C. Gao, W. Li, X. Chen, X. Chen, P. Sun, Y. Dong, Z. Cai and Z. He, Multi-Functional Integration of Phosphor, Initiator, and Crosslinker for the Photo-Polymerization of Flexible Phosphorescent Polymer Gels, *Angew. Chem., Int. Ed.*, 2024, **63**, e202401331.
  - 22 N. Li, X. Yang, B. Wang, P. Chen, Y. Ma, Q. Zhang, Y. Huang, Y. Zhang and S. Lü, Color-tunable Room-temperature Phosphorescence from Non-aromatic-polymer-involved Charge Transfer, *Adv. Sci.*, 2024, **11**, 2404698.
  - 23 L. Gao, J. Huang, L. Qu, X. Chen, Y. Zhu, C. Li, Q. Tian, Y. Zhao and C. Yang, Stepwise Taming of Triplet Excitons via Multiple Confinements in Intrinsic Polymers for Long-lived Room-temperature Phosphorescence, *Nat. Commun.*, 2023, **14**, 7252.
  - 24 S. Tang, S. Jiang, K. Wang, Y. Zhang, L. Yi, J. Hou, L. Qu, Y. Zhao and C. Yang, Cycloolefin Copolymers With a Multiply Rigid Structure for Protecting Triplet Exciton From Thermo- and Moisture-Quenching, *Adv. Mater.*, 2025, **37**, 2416397.
  - 25 W. Zhao, T. S. Cheung, N. Jiang, W. Huang, J. W. Y. Lam, X. Zhang, Z. He and B. Z. Tang, Boosting the Efficiency of Organic Persistent Room-Temperature Phosphorescence by Intramolecular Triplet-Triplet Energy Transfer, *Nat. Commun.*, 2019, **10**, 1595.
  - 26 R. Zhang, B. Yuan, F. Pan, H. Liang, H. Jiang, H. Guo, Y. Rao, S. Zheng, L. Ruan, C. Wu, Y. Yang and W. Lu, Ultratransparent, Stretchable, and Durable Electromagnetic Wave Absorbers, *Matter*, 2025, **8**, 101956.
  - 27 C. Wei, L. Bai, X. An, M. Xu, W. Liu, W. Zhang, M. Singh, K. Shen, Y. Han, L. Sun, J. Lin, Q. Zhao, Y. Zhang, Y. Yang, M. Yu, Y. Li, N. Sun, Y. Han, L. Xie, C. Ou, B. Sun, X. Ding, C. Xu, Z. An, R. Chen, H. Ling, W. Li, J. Wang and W. Huang, Atomic-Resolved Hierarchical Structure of Elastic  $\pi$ -Conjugated Molecular Crystal for Flexible Organic Photonics, *Chem*, 2022, **8**, 1427–1441.
  - 28 K. Chen, Y. Zhang, Y. Lei, W. Dai, M. Liu, Z. Cai, H. Wu, X. Huang and X. Ma, Twofold Rigidity Activates Ultralong Organic High-Temperature Phosphorescence, *Nat. Commun.*, 2024, **15**, 1269.
  - 29 X. Yao, J. Wang, D. Jiao, Z. Huang, O. Mhirs, F. Lossada, L. Chen, B. Haehnle, A. J. C. Kuehne, X. Ma, H. Tian and A. Walther, Room-Temperature Phosphorescence Enabled through Nacre-Mimetic Nanocomposite Design, *Adv. Mater.*, 2020, **33**, 2005973.
  - 30 L. Zhou, J. Song, Z. He, Y. Liu, P. Jiang, T. Li and X. Ma, Achieving Efficient Dark Blue Room-Temperature Phosphorescence with Ultra-Wide Range Tunable-Lifetime, *Angew. Chem., Int. Ed.*, 2024, **63**, e202403773.
  - 31 Y. Miao, F. Lin, D. Guo, J. Chen, K. Zhang, T. Wu, H. Huang, Z. Chi and Z. Yang, Stable and Ultralong Room-Temperature Phosphorescent Copolymers with Excellent Adhesion, Resistance, and Toughness, *Sci. Adv.*, 2024, **10**, eadk3354.
  - 32 J. Zhang, S. Zhang, C. Sun, R. Wang, Z. Guo, D. Cui, G. Tang, D. Li, J. Yuan, X. Lu, C. Zheng, W. Huang and R. Chen, Highly Bright Pure Room Temperature Phosphorescence for Circularly Polarized Organic Hyperafterglow, *Adv. Mater.*, 2025, **37**, 2500953.
  - 33 Y. Huang, Y. Liu, X. Zheng, J. Wu, Q. Ling and Z. Lin, Internal Locking and External Anchoring—A Strategy for Constructing Efficient and Ultralong Room-Temperature Phosphorescence Materials, *Adv. Opt. Mater.*, 2025, **13**, 2500743.
  - 34 Y. Zhou, P. Zhang, Z. Liu, W. Yan, H. Gao, G. Liang and W. Qin, Sunlight-Activated Hour-Long Afterglow from

- Transparent and Flexible Polymers, *Adv. Mater.*, 2024, **36**, e2312439.
- 35 Z. Lin, R. Kabe, N. Nishimura, K. Jinnai and C. Adachi, Organic Long-Persistent Luminescence from a Flexible and Transparent Doped Polymer, *Adv. Mater.*, 2018, **30**, e1803713.
- 36 N. Gan, X. Zou, Z. Qian, A. Lv, L. Wang, H. Ma, H.-J. Qian, L. Gu, Z. An and W. Huang, Stretchable Phosphorescent Polymers by Multiphase Engineering, *Nat. Commun.*, 2024, **15**, 4113.
- 37 W. Gao, D. Li, H. Feng and Z. Su, Stretchable Organic Room Temperature Phosphorescence Systems, *J. Mater. Chem. C*, 2025, **13**, 13607–13619.
- 38 Z. Sun, H. Deng, Z. Mao, Z. Li, K. Nie, K. Fu, J. Chen, J. Zhao, P. Zhu, Z. Chi and R. Sun, Shape-Memorable, Self-Healable, Recyclable, and Full-Color Emissive Ultralong Organic Phosphorescence Vitrimers with Exchangeable Covalent Bonds, *Adv. Opt. Mater.*, 2022, **10**, 2201558.
- 39 J. Wei, M. Zhu, T. Du, J. Li, P. Dai, C. Liu, J. Duan, S. Liu, X. Zhou, S. Zhang, L. Guo, H. Wang, Y. Ma, W. Huang and Q. Zhao, Full-Color Persistent Room Temperature Phosphorescent Elastomers with Robust Optical Properties, *Nat. Commun.*, 2023, **14**, 4839.
- 40 M. Yao, W. Wei, W. Qiao, Y. Zhang, X. Zhou, Z. A. Li, H. Peng and X. Xie, High-Security Plastic with Integrated Holographic and Phosphorescent Images, *Adv. Mater.*, 2025, **37**, e2414894.
- 41 L. Qiu, Z. Chen, J. Wu, G. Zeng, X. Liu, K. Liu, S.-J. Su, J. Loos and T. Wen, Room-Temperature Phosphorescence Induced by Heterogeneous Polymer Matrixes, *Macromolecules*, 2024, **57**, 2679–2686.
- 42 H. Chen, Z. Qian, H. Qian, M. Dong, Y. Zhang, J. Shan, W. Huo, A. Lv, J. Guo, H. Ma, Z. An, W. Huang and L. Gu, Stretchable and Flexible Room-Temperature Phosphorescence Copolymers Based on Microphase Separation, *Chem. Mater.*, 2024, **36**, 5100–5109.
- 43 Y. Zhang, Q. Sun, L. Yue, Y. Wang, S. Cui, H. Zhang, S. Xue and W. Yang, Room Temperature Phosphorescent (RTP) Thermoplastic Elastomers with Dual and Variable RTP Emission, Photo-Patterning Memory Effect, and Dynamic Deformation RTP Response, *Adv. Sci.*, 2022, **9**, 2103402.
- 44 H. Ju, H. Zhang, L. Hou, M. Zuo, M. Du, F. Huang, Q. Zheng and Z. Wu, Polymerization-Induced Crystallization of Dopant Molecules: An Efficient Strategy for Room-Temperature Phosphorescence of Hydrogels, *J. Am. Chem. Soc.*, 2023, **145**, 3763–3773.
- 45 B. Chu, H. Zhang, L. Hu, B. Liu, C. Zhang, X. Zhang and B. Z. Tang, Altering Chain Flexibility of Aliphatic Polyesters for Yellow-Green Clusteroluminescence in 38% Quantum Yield, *Angew. Chem., Int. Ed.*, 2022, **61**, e202114117.
- 46 X. Chen, W. Luo, H. Ma, Q. Peng, W. Z. Yuan and Y. Zhang, Prevalent Intrinsic Emission from Nonaromatic Amino Acids and Poly(amino acids), *Sci. China: Chem.*, 2018, **61**, 351–359.
- 47 X. Huang, Y. Zhang, G. Li, T. Wang, P. Sun, J. Shi, B. Tong, J. Zhi, Z. Li, Z. Cai and Y. Dong, Recent Progress of Organic Room-Temperature Phosphorescent Hydrogels, *ChemPhotoChem*, 2025, **9**, e202400315.
- 48 J. Chen, F. Lin, D. Guo, T. Tang, Y. Miao, Y. Wu, W. Zhai, H. Huang, Z. Chi, Y. Chen and Z. Yang, In Situ Reversible and Robust Mechano-Responsive Ultralong Phosphorescence of Polyurethane Elastomer, *Adv. Mater.*, 2024, **36**, 2409642.
- 49 J. Chen, Y. Zhang, S. Zhang, G. Liu, Q. Sun, S. Xue and W. Yang, Two-Phase Rubber–Plastic Matrices' Stabilization of Organic Room-Temperature Phosphorescence Afterglows Better than Plastic Matrix, *Small Struct.*, 2023, **4**, 2300101.
- 50 J. Liu, Z. Song, J. Wei, J. Wu, M. Wang, J. Li, Y. Ma, B. Li, Y. Lu and Q. Zhao, Circularly Polarized Organic Ultralong Room-Temperature Phosphorescence with A High Dissymmetry Factor in Chiral Helical Superstructures, *Adv. Mater.*, 2024, **36**, 2306834.
- 51 Z. Song, J. Wei, J. Liu, Z. Chu, J. Hu, S. Chakraborty, Y. Ma, B. Li, Y. Lu and Q. Zhao, Mechanically-Tunable and Full-Color Circularly Polarized Long-Lived Phosphorescence in Chiral Superstructure Elastomers, *Adv. Mater.*, 2025, **37**, 2419640.
- 52 J. Huang, L. Qu, L. Gao, X. Wang, Q. Chen, Y. Wang, Y. Zhu, C. Li, Y. Li and C. Yang, Multicolor Room-Temperature Phosphorescence Achieved by Intrinsic Polymers Containing Solely One Phosphor Unit, *Macromolecules*, 2024, **57**, 5018–5027.
- 53 P. Chen, H. Qie, X. Yang, S. Ma, Z. Wang, N. Li, Y. Deng, F. Bian and S. Lü, Luminous Fish-Inspired Hydrogels with Underwater Long-Lived Room Temperature Phosphorescence, *Adv. Funct. Mater.*, 2025, **35**, 2416430.
- 54 J. Guo, C. Yang and Y. Zhao, Long-Lived Organic Room-Temperature Phosphorescence from Amorphous Polymer Systems, *Acc. Chem. Res.*, 2022, **55**, 1160–1170.
- 55 B. Ding, X. Ma and H. Tian, Recent Advances of Pure Organic Room Temperature Phosphorescence Based on Functional Polymers, *Acc. Mater. Res.*, 2023, **4**, 827–838.
- 56 X. Luo, B. Tian, Y. Zhai, H. Guo, S. Liu, J. Li, S. Li, T. D. James and Z. Chen, Room-Temperature Phosphorescent Materials Derived from Natural Resources, *Nat. Rev. Chem.*, 2023, **7**, 800–812.
- 57 F. Guo, Y. Chen, C. Li, X. Wang, Q. Li, M. He, H. Hou and C. Yang, Visualization Detection of Ultralow Temperature Based on Flexible Cross-linked Polymer Systems, *Adv. Funct. Mater.*, 2025, **35**, 2416465.